

# Molecular Mobility of Peroxy Radicals at the Ends of Isolated Polystyrene Chains Tethered on the Solid Surface of Poly(tetrafluoroethylene) in a Vacuum

Masato Sakaguchi,<sup>\*,†</sup> Katsuhiko Yamamoto,<sup>‡</sup> Yohei Miwa,<sup>‡</sup> Shigetaka Shimada,<sup>‡</sup> Masahiro Sakai,<sup>§</sup> and Takeru Iwamura<sup>†</sup>

*Institute for Environmental Sciences, University of Shizuoka, 52-1, Yada, Suruga-ku, Shizuoka 422-8526, Japan; Department of Materials Science & Engineering, Nagoya Institute of Technology, Gokiso-cho, Showa-ku, Nagoya 466-8555, Japan; and Research Center for Molecular-Scale Nanoscience, Institute for Molecular Science, 38, Nishigo-Naka, Myodaiji, Okazaki 4444-8585, Japan*

*Received October 26, 2006; Revised Manuscript Received December 9, 2006*

**ABSTRACT:** The molecular mobility of peroxy radicals at the ends of isolated polystyrene chains (IPSOO) tethered on the solid surface of poly(tetrafluoroethylene) (PTFE) was investigated in a vacuum in the temperature range from 10 to 250 K by electron spin resonance spectroscopy. The onset of an anisotropic tumbling motion of IPSOO at a train state on the PTFE surface was 80 K. When the temperature was above 150 K, the IPSOO protruded from the PTFE surface and resulted in a tail state, in which the IPSOO was in a free rotational state. A train–tail transition temperature was defined at 160 K, which was extremely low compared to the glass transition temperature (373 K) of polystyrene (PS) in the bulk. The activation energy of the IPSOO of the tail state was calculated as 8.3–9.2 kJ/mol. The remarkably high mobility and low activation energy of the IPSOO are probably due to an isolated chain on the PTFE surface, a low chain segmental density, a chain end, and a weak interaction with the PTFE surface.

## Introduction

Many investigations have been conducted on the mobility of polymer chains in the bulk. They indicate that the mobility of polymer chains strongly depends on their surroundings, which is composed of polymer chains and a free volume. The mobility relates to the amount and size of the free volume in the surroundings. Recently, some research groups focused on a mobility of chains on the surface of polymeric materials due to its importance in various practical applications such as adhesives and lubricants and so on. Forrest and co-workers<sup>1–3</sup> have reported that a glass transition temperature ( $T_g$ ) for freely standing films was reduced below the bulk value and decreased linearly with film thickness. Theodorou and co-workers<sup>4</sup> have reported that the center-of-mass motion of chains located near the surface was enhanced compared to that in the bulk polymer, which was revealed by molecular dynamics computer simulations. Ngai and co-workers<sup>5</sup> have reported that dramatic reduction of  $T_g$  in freely standing polymer thin films was due to decrease of the cooperative length scale for chain segments near the surface. Mattice and co-workers<sup>6</sup> have reported that the mobility of chains increased toward the free surfaces due to decrease in density, which was revealed by coarse-grained simulations of thin polyethylene films. Kajiyama and co-workers<sup>7–11</sup> have reported that a glass transition temperature at the surface ( $T_g^s$ ) of polystyrene (PS) film was lower than the temperature in the bulk ( $T_g^b$ ) using a scanning atomic force microscope. The reduction of  $T_g^s$  of PS film surface was attributed to the excess free volume generated by the chain ends at the surface.<sup>8,10,11</sup> The excess free volume led to a decrease in

chain segmental density at the surface and promoted chain activity.

Electron spin resonance spectroscopy (ESR) can detect and assign radical species. Furthermore, molecular motion of polymer chains having radicals can be evaluated by using a spectral simulation. Authors have systematically studied surface molecular motion of polymer chains by mainly using ESR.<sup>12–21</sup> We earlier indicated that the mobility of any polymer chain tethered on the surface was higher than that in the bulk. The high mobility was associated with the extremely low density of the chains on the surface. In addition, we found that an isolated single chain had high mobility. For example, the site exchange motion of isolated polyethylene chain-end radicals tethered on the surface of poly(tetrafluoroethylene) (PTFE) in a vacuum occurred at 2.6 K,<sup>18</sup> and the free rotation of the chain ends occurred at 95 K.<sup>16</sup>

It is well-known that different radical species reveal different ESR spectra. When any type of alkyl radical converts to a peroxy radical, the peroxy radical at a rigid limit motion reveals almost the same spectrum in a powder pattern. A spectral change of peroxy radical reflects its molecular mobility. Therefore, the molecular mobility can be directly analyzed from spectral changes. In a previous study, we reported<sup>19</sup> that train–tail transition temperatures of peroxy end-radicals of polymers tethered on the PTFE surface—polyethylene (PE) (123 K), polybutadiene (PB) (142 K), polypropylene (PP) (145 K), polyisobutylene (PIB) (174 K), and poly(methyl methacrylate) (PMMA) (253 K)—and all these transition temperatures were lower than those of  $T_g$  in the bulk. Unfortunately, we could not evaluate the molecular dynamics parameters such as motional correlation time and activation energy of the motion due to limitation of our computer simulation program.

This article reports that a motional correlation time and its activation energy of peroxy radicals at the ends of isolated polystyrene chains tethered on the solid surface of PTFE in a

\* Corresponding author: e-mail sakaguchi@u-shizuoka-ken.ac.jp, phone +81-54-264-5786, Fax +81-54-264-5786.

<sup>†</sup> University of Shizuoka.

<sup>‡</sup> Nagoya Institute of Technology.

<sup>§</sup> Institute for Molecular Science.

vacuum were evaluated by spectral simulations, and the mobility of the ends of the isolated polystyrene chains was extremely high compared to that in the bulk.

## Experimental Section

PTFE (Fluon G163, Asahi Glass Co., Ltd.) was used without further purification. Inhibitor in styrene (St, Cica pure reagent, Kanto Chemical Co., Ltd.) was adsorbed to activated aluminum oxide (particle size 2–4 mm, Kanto Chemical Co., Ltd.) and removed. St was purified by distilling twice in a vacuum line. Oxygen gas included in St was eliminated by four repeat times of the freeze–pump–thaw method.

The PS chains tethered on the solid surface of PTFE in a vacuum were produced by the same procedure as described in the previous reports from our laboratory.<sup>13,16,19,21,23</sup> The following procedure was used: The solid PTFE (1.5 g) in a glass-ball-mill connected to a vacuum line was evacuated under 0.6 Pa at 353 K for 4 h. The purified St ( $1.2 \times 10^{-5}$  mol) was introduced into the glass ball mill in a vacuum line. The glass ball mill containing solid PTFE and St was sealed off from the vacuum line, and set in a vessel filled with liquid nitrogen. The solid sample of PTFE and St in the glass ball mill was mechanically fractured by a homemade vibration ball mill apparatus<sup>24</sup> for 21 h at 77 K in a vacuum. After milling, the powdered sample was dropped into an ESR sample tube attached to the top of the glass ball mill.

ESR spectra were observed at a microwave power level of 0.1 mW to avoid power saturation and with 100 kHz field modulation using a Bruker ESP300E spectrometer (X-band) equipped with a helium cryostat (Oxford ESR 900) and a temperature controller (Oxford ITC4). Before ESR observation, the sample was cooled to 4 K in the cryostat and kept for 1 h. The sample was kept at elevated temperature for 15 min, and then ESR spectra were observed at the temperature.

We have modified Heinzer's method<sup>25</sup> to calculate a line-shape equation of ESR spectra in the solid state having anisotropic  $\mathbf{g}$  and hyperfine splitting tensors  $\mathbf{A}$ . As has been shown in a previous paper,<sup>21</sup> the complex magnetization,  $Z$ , is given by

$$Z = -iCS^{-1} \sum_{j=1}^{n_L} D_j \mathbf{M}_{0j}^{-1} \mathbf{P} \quad (1)$$

According to Heinzer's definition,  $\mathbf{M}_0$  is a complex non-hermitian matrix of dimension  $N = n_C n_L$ , with  $n_C$  = number of chemical configurations and  $n_L$  = number of lines.  $\mathbf{P}$  is a population, and  $\mathbf{S}^{-1}$  is shift operator. The degeneracy of a transition is denoted by  $D_j$ . The  $C$  denotes a scaling factor. The imaginary part of  $Z$  yields the absorption line shape equation directly.  $\mathbf{M}_{0j}$  can be decomposed into a constant matrix,  $\mathbf{F}$ , and a scalar matrix,  $i\mathbf{H}\mathbf{E}$ , which are exhibited with a magnetic field unit instead of a frequency unit:

$$\mathbf{M}_{0j} = \mathbf{F}_j + i\mathbf{H}\mathbf{E}$$

with

$$\mathbf{F}_j = \sum_{r=1}^{n_C} \sum_{s=1}^{n_C} [-i\delta_{rs}(H^\circ_r + \sum_{\alpha=1}^{n_A} A_{r\alpha}) - \delta_{rs}(1/T_2) - \delta_{rs} \sum_{m \neq r}^{n_C} K_m + (1 - \delta_{rs})K_{sr}]$$

$$K_{sr} = (1/\tau_r)(h/2\pi)\omega_{0,r}/(g_r\beta)$$

$$1/T_2 = (1/T_{2,r})(h/2\pi)\omega_r/(g_r\beta)$$

$$H^\circ_r = (h/2\pi)\omega_r/(g_r\beta)$$

$$g_r^2 = g_{r1}^2 \cos^2 \phi \sin^2 \theta + g_{r2}^2 \sin^2 \phi \sin^2 \theta + g_{r3}^2 \cos^2 \theta$$

$$A_r^2 = A_{r1}^2 \cos^2 \phi \sin^2 \theta + A_{r2}^2 \sin^2 \phi \sin^2 \theta + A_{r3}^2 \cos^2 \theta$$

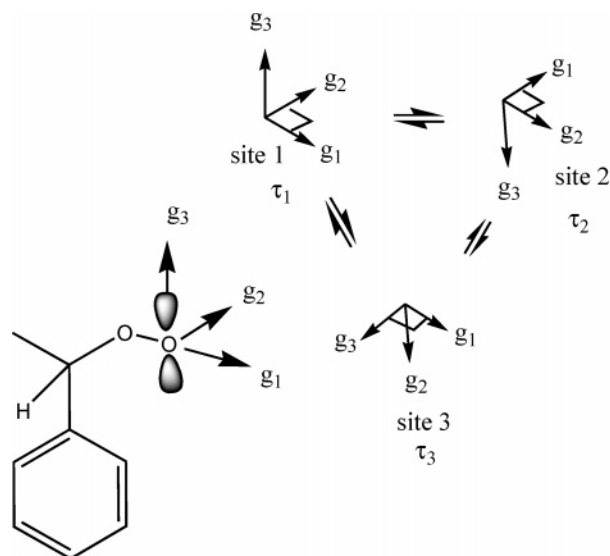
$K_{sr}$  is treated as the rate of conformation change from  $r$  to  $s$ .  $\tau_r$  is a correlation time denoted by a residence time of  $r$  conformation.  $H^\circ_r$  is an electronic Zeeman interaction of  $r$  conformation.  $1/T_2$  is a line width. The  $g_r$  and  $A_r$  are  $g$  values and hyperfine splitting constant at the  $r$  conformation. The last two terms,  $-\delta_{rs} \sum_{m \neq r}^{n_C} K_m + (1 - \delta_{rs})K_{sr}$ , are responsible for the intramolecular exchange.

The coordinate system of a peroxy radical revealing the principal direction of the  $\mathbf{g}$  tensor is shown in Figure 1. Site 1 is defined as the direction of the  $g_1$  (2.0355) axis (that is, the direction of the maximum principal value)<sup>26,27</sup> which is parallel to the axis of the oxygen–oxygen bond, the direction of the  $g_3$  (2.0023) axis (that is, the direction of the minimum principal value)<sup>26,27</sup> parallel to the direction of the p orbital and perpendicular to the C–O–O plane, and the  $g_2$  (2.0080) axis which is perpendicular to both the  $g_1$  and  $g_3$  axes. Two other sites were defined as follows: site 2 (2.0080, 2.0355, 2.0023) and site 3 (2.0355, 2.0023, 2.0080). In our spectral simulation, we assumed that a peroxy radical stayed at site  $r$  with a correlation time  $\tau_r$  and then jumped to another site. The correlation time without distribution was assumed. The Gaussian distribution function was employed as a line shape function.

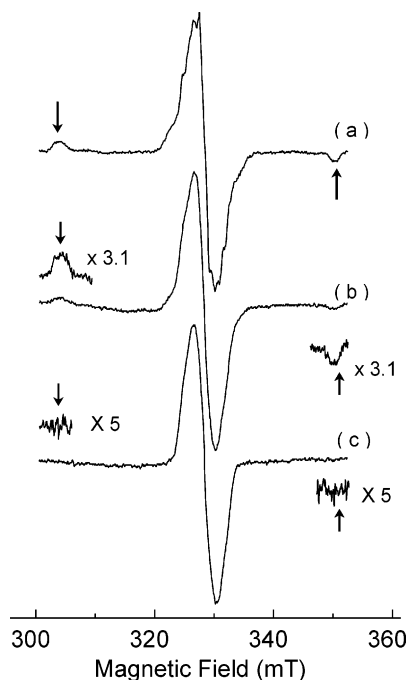
## Results and Discussion

Figure 2a shows the ESR spectrum observed at 77 K of PTFE milled with St in a vacuum at 77 K. The spectrum reveals the characteristic wing peaks (shown with arrows) on the outer parts of the spectrum having a hyperfine splitting constant of 45.7 mT, which is assigned to the spectrum due to the radicals having two  $\alpha$  F atoms.<sup>24</sup> Thus, the spectrum indicates that PTFE mechano radicals and chain end-type radicals,  $-\text{CF}_2-\text{CF}_2^\bullet$ , were produced by the milling of PTFE. After annealing at 193 K for 8 min, the wing peaks decreased (shown with arrows in Figure 2b) and disappeared by annealing at 233 K for 10 min (shown with arrows in Figure 2c). With the annealing procedure, the central peak became a smoothed line, and the line width increased from 3.11 to 3.84 mT. We have reported that mechano radicals were localized on the fresh surface of fractured polymers.<sup>28,29</sup> The PTFE mechano radicals could initiate a radical polymerization of several monomers, such as ethylene,<sup>13,21</sup> methyl methacrylate,<sup>22</sup> isobutylene,<sup>30</sup> and 1,3-butadiene.<sup>31</sup> Furthermore,  $g$  values of the observed peroxy radical of PS are greater than those of PTFE, which is indicated in a later section. Thus, the singlet spectrum of Figure 2c can be assigned to PS propagating radicals.

Assuming no residue of St monomer, the average degree of polymerization (DP) of PS was calculated as 72 by the concentrations of St ( $1.2 \times 10^{-5}$  mol) and PTFE mechano radicals ( $6.8 \times 10^{16}$  radicals/g) located on the surface of PTFE.<sup>13</sup> The radius of gyration ( $R_g = (C_\infty (2DP - 1)a_b^2/6)^{0.5}$ ) of PS was calculated as 2.4 nm on the basis of the 72 of DP, carbon–carbon bond length ( $a_b = 0.15351$  nm),<sup>32</sup> and characteristic ratio ( $C_\infty = 10.46$ ) of atactic PS.<sup>33</sup> The area per tethered point on the PTFE surface was calculated as 31 nm<sup>2</sup> on the basis of the concentration of PTFE mechano radicals located on the surface and specific surface area (2.1 m<sup>2</sup>/g).<sup>13</sup> Assuming the area of a circle as 31 nm<sup>2</sup>, the radius ( $R_t$ ) per tethered point is 3.1 nm. Since a relative radius ( $R_L = R_g/R_t$ ) of PS having 72 DP is 0.77, a tethered PS chain cannot contact and entangle with neighboring PS chains. Each PS chain cannot aggregate because the chain is tethered on the PTFE surface by a covalent bond. PS is immiscible with PTFE. Therefore, the tethered PS chain can be regarded as an “isolated PS chain” (IPS).



**Figure 1.** Coordinate system of peroxy radical revealing principal direction of  $\mathbf{g}$  tensor ( $g_1 = 2.0355 \pm 0.00005$ ,  $g_2 = 2.0080 \pm 0.00005$ , and  $g_3 = 2.0023 \pm 0.00005$ ): Site 1 is defined as the direction of  $g_1$  (2.0355) axis is parallel to the axis of the oxygen–oxygen bond, the direction of  $g_3$  (2.0023) axis is parallel to the direction of the p orbital and perpendicular to the C–O–O plane and, and  $g_2$  (2.0080) axis is perpendicular to both  $g_1$  and  $g_3$  axes. Site 2: (2.0080, 2.0355, 2.0023); site 3: (2.0355, 2.0023, 2.0080).



**Figure 2.** ESR spectral change with advancing the polymerization reaction from PTFE chain-end radicals to IPS radicals: (a) as-fractured PTFE with St monomer at 77 K; (b) annealing at 193 K for 8 min; (c) annealing at 233 K for 10 min. Arrows indicate the wing peaks due to the radicals of  $-\text{CF}_2\text{CF}_2^\bullet$ . All spectra were observed at 77 K.

On this stage, the IPS chain has a free radical at the terminal of the chain because the IPS chain is a propagating radical. The IPS chains were contacted to oxygen molecules at 77 K. After contact, ESR spectrum changed from the singlet spectrum to the spectrum with humps on the shoulder (shown in Figure 3a with arrows), which corresponded to  $g_1 = 2.0355$  and  $g_2 = 2.0023$ . After annealing at 193 K for 8 min, the ESR spectrum observed at 77 K was drastically changed and showed a powder pattern of peroxy radicals, in which a molecular motion of the radicals was frozen (Figure 3b). Hereafter, the ends of peroxy

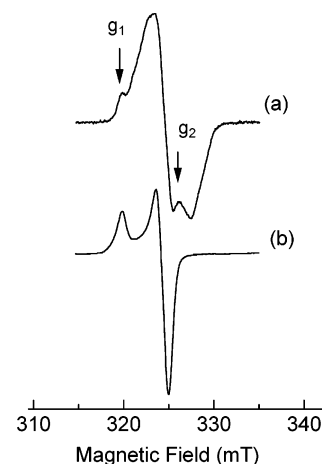


**Figure 3.** Spectral change with advancing the oxidation reaction from the chain end-type alkyl radicals at the ends of IPS to the peroxy radicals: (a) after contact with oxygen molecules at 77 K; (b) after annealing at 193 K for 8 min. All spectra were observed at 77 K. Arrows show  $g$  values:  $g_1 = 2.0355$ ,  $g_2 = 2.0023$ .

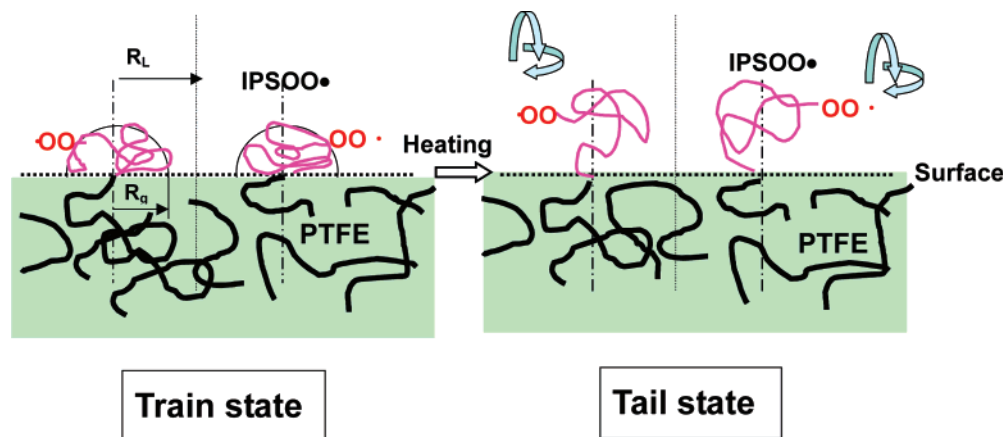
radicals of IPS chains tethered on the solid surface of PTFE are called “peroxy ends of the isolated PS chains” (IPSOO). The IPSOO is located on the PTFE surface and may have a mushroom shape induced from extremely low chain segmental density (illustrated in Figure 4, train state).

Temperature-dependent ESR spectra of IPSOO observed in the temperature range from 10 to 250 K are shown in Figure 5 with solid lines. The spectrum observed at 10 K is a characteristic powder pattern of a frozen molecular motion. The simulated spectrum at 10 K using the three principal values of  $\mathbf{g}$  tensor ( $g_1 = 2.0355 \pm 0.00005$ ,  $g_2 = 2.0080 \pm 0.00005$ , and  $g_3 = 2.0023 \pm 0.00005$ ) in a frozen molecular motion, a rigid-limit model, is in good agreement with the observed spectrum (shown in Figure 5 at 10 K with broken line). On the other hand, we have reported that  $g$  values of peroxy radicals of PTFE were  $g_1 = 2.0429$ ,  $g_2 = 2.0081$ ,  $g_3 = 2.0018$ , and  $g_{\text{iso}} = 2.0176$ .<sup>14</sup> These values are not identical with those of  $g_1 = 2.0355$  and  $g_{\text{iso}} = 2.0153$  of the IPSOO. Accordingly, these results strongly suggest that PS propagating radicals converted to PS peroxy radicals.

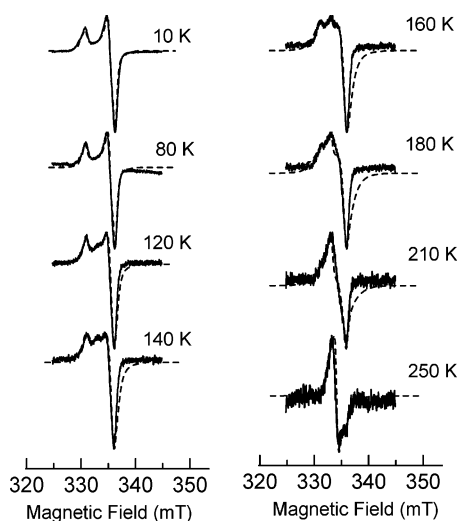
Although the shape of the spectrum observed at 80 K is almost the same as that observed at 10 K, the depth of the valley between the signal position of  $g_1$  and  $g_2$  slightly decreased in relation to that observed at 10 K. The decrease suggests that a small-scale motion occurs at the temperature. The simulated spectrum of 80 K is in good agreement with the observed spectrum, which was calculated using the  $g$  values of the rigid limit model and an isotropic correlation time,  $\tau_1 = \tau_2 = \tau_3 = (1.0 \pm 0.2) \times 10^{-7}$  s. The isotropic correlation time corresponds to the same residence time in each site and reveals an isotropic motional mode. Spectra registered at the elevated temperatures at which ESR spectra were simulated were calculated using the same principal  $g$  values, except for each correlation time (shown in Figure 5 with broken lines). The spectral change of IPSOO with increasing temperature is due to molecular motion of IPSOO with corresponding correlation time. Anisotropic correlation times at 100 K were calculated as  $\tau_1 = \tau_2 = (4.4 \pm 0.1) \times 10^{-8}$  s corresponding to a short correlation time and  $\tau_3 = (6.4 \pm 0.1) \times 10^{-8}$  s corresponding to a long correlation time. The anisotropic motion of IPSOO corresponding to long and short correlation times increased with increasing temperature (Figure 6).

Figure 6 shows Arrhenius plots of  $\tau$  of IPSOO vs inverse temperature. The long and short correlation times are shown





**Figure 4.** Schematic illustration of IPSOO chains on the PTFE surface, which take a train conformation below 150 K and a tail conformation at above 150 K.  $R_g$  = radius of gyration;  $R_L = R_g/R_t$ , a relative radius to a radius of a tethered point,  $R_t$ .



**Figure 5.** Temperature-dependent ESR spectra of IPSOO on PTFE surface. Observed spectra are shown with solid lines, and simulated spectra are shown with broken lines. Simulation spectra were calculated using the three  $g$  values ( $2.0355 \pm 0.00005$ ,  $2.0080 \pm 0.00005$ ,  $2.0023 \pm 0.00005$ ) and each correlation time.

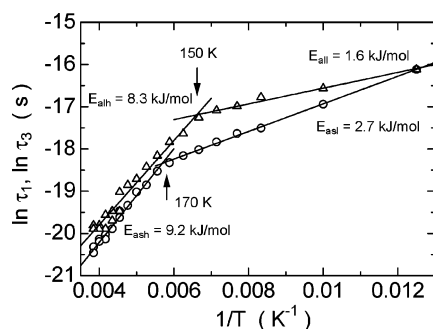


**Figure 6.** Arrhenius plot of correlation time  $\tau$  of IPSOO vs inverse temperature: circles, short correlation time  $\tau_1$ ; triangles, long correlation time  $\tau_3$ .  $E_{all}$  and  $E_{ah}$  are activation energies of a long correlation time in temperature ranges from 80 to 150 K and from 150 to 250 K.  $E_{asl}$  and  $E_{ash}$  are activation energies in temperature ranges from 80 to 170 K and from 170 to 250 K.

with triangles and circles. The long correlation time decreases with temperature increasing and steeply decreases above 150 K. The activation energy ( $E_{all}$ ) of the motion was  $1.6 \pm 0.2$  kJ/mol, which was derived from the slope of the line depicted by the least-squares method in the temperature range from 80 to 150 K. The short correlation time also decreases with temperature increasing but steeply decreasing point shifts to 170

K. The activation energy ( $E_{asl}$ ) in the temperature range from 80 to 170 K was calculated as  $2.7 \pm 0.2$  kJ/mol. The values of  $E_{all}$  and  $E_{asl}$  are very small and almost identical. Thus, the corresponding motional mode of IPSOO may be a small-scale motion with an anisotropic tumbling motion on the PTFE surface or a motion by a tunnel effect. When the observation temperature was above 150 K, the long correlation times steeply decrease with temperature increasing. The activation energy ( $E_{ah}$ ) in the temperature range from 150 to 250 K was estimated as  $8.3 \pm 0.2$  kJ/mol. For the short correlation time, its activation energy ( $E_{ash}$ ) in the temperature range from 170 to 250 K was  $9.2 \pm 0.2$  kJ/mol. The  $E_{ah}$  and  $E_{ash}$  are almost the same value. Since the difference between  $\tau_3$  and  $\tau_1$  decreased over 150 K, the anisotropic motional mode changed into a less anisotropic one above 150 K (Figure 6). Both the small anisotropy between the short and long correlation times and the close activation energy suggest a similar motional mode above 150 K. The ESR shape with correlation time  $(1.5 \pm 0.1) \times 10^{-9}$  s at 250 K reveals that IPSOO is a characteristic free rotational state. Thus, the IPSOO chain probably protrudes from the PTFE surface and rotates freely. This indicates a motional transition from a train state to a tail state. The train–tail motional transition temperature is defined at 160 K due to the midpoint of the two alteration points of 150 and 170 K. The 20 K difference of the alteration points 150 and 170 K corresponding to long and short correlation times, respectively, cannot be explained obviously. However, a motional mode with a long correlation time corresponding to a slow motion may be activated in a lower temperature range to achieve the train–tail transition. The transition temperature of 160 K is extremely low compared to the glass transition temperature of PS (373 K)<sup>34</sup> in the bulk and that of the surface of ultrathin film (341 K).<sup>35</sup> Furthermore, the activation energy of IPSOO is remarkably low compared to the activation energy ( $230 \pm 10$  kJ/mol) of the surface segmental motion in the PS film.<sup>36</sup>

Another point of view is the free rotational motion of IPSOO based on only activation energy (8.3–9.2 kJ/mol) may correspond to a molecular motion based on a rotational isomeric state model, which is based on an intrinsic 3-fold torsion potential having a barrier height of 11.7 kJ/mol assigned to each skeletal C–C bond.<sup>37,38</sup> On the other hand, the activation energy of 8.3–9.2 kJ/mol of IPSOO corresponds to that of 9.0–18.0 kJ/mol of spin-labeled PS with nitroxide radical in dilute toluene solution.<sup>39</sup> Freed and co-workers reported that the activation energy of spin-labeled polystyrene in dilute toluene solution by using the ESR technique is  $11.9 \pm 1.5$  kJ/mol, which is in good agreement with results from fluorescence studies.<sup>40</sup> Therefore,

it is strongly suggested that the mobility of IPSOO corresponds to the mobility in a dilute toluene solution, in which PS chains are isolated from neighboring PS chains.

## Conclusions

The molecular mobility of IPSOO tethered on the solid surface of PTFE in a vacuum was investigated in the temperature range from 10 to 250 K by ESR. It was found that the onset of an anisotropic tumbling motion of IPSOO on the PTFE surface at a train state was 80 K. Above 150 K, the IPSOO protruded from the PTFE surface and resulted in a free rotational state, a tail state. The activation energy of the IPSOO of the tail state was calculated as 8.3–9.2 kJ/mol. The remarkably high mobility and low activation energy of the IPSOO are probably due to an isolated chain on the PTFE surface, a low chain segmental density, a chain end, and a weak interaction with the PTFE surface.

## References and Notes

- (1) Forrest, J. A.; Dalnoki-Veress, K.; Stevens, J. R.; Dutcher, J. R. *Phys. Rev. Lett.* **1996**, *77*, 2002.
- (2) Forrest, J. A.; Dalnoki-Veress, K.; Stevens, J. R.; Dutcher, J. R. *Phys. Rev. E* **1997**, *56*, 5705.
- (3) Forrest, J. A.; Svanberg, C.; Revesz, K.; Rodahl, M.; Torell, L. M.; Kasemo, B. *Phys. Rev. E* **1998**, *58*, R1226.
- (4) Mansfield, K. F.; Theodorou, N. *Macromolecules* **1991**, *24*, 6283.
- (5) Ngai, K. L.; Rzos, A. K.; Plazek, D. J. *J. Non-Cryst. Solids* **1998**, *235–237*, 435.
- (6) Doruker, P.; Mattice, W. L. *Macromolecules* **1999**, *32*, 194.
- (7) Kajiyama, T.; Tanaka, K.; Takahara, A. *Macromolecules* **1997**, *30*, 280.
- (8) Satomi, N.; Takahara, A.; Kajiyama, T. *Macromolecules* **1999**, *32*, 4474.
- (9) Kawaguchi, D.; Tanaka, K.; Takahara, A.; Kajiyama, T. *Macromolecules* **2001**, *34*, 6164.
- (10) Kawaguchi, D.; Tanaka, K.; Takahara, A.; Kajiyama, T.; Takahara, A.; Tadaki, S. *Macromolecules* **2003**, *36*, 1235.
- (11) Tanaka, K.; Takahara, A.; Kajiyama, T. *Macromolecules* **2000**, *33*, 7588.
- (12) Sakaguchi, M.; Yamaguchi, T.; Shimada, S.; Hori, Y. *Macromolecules* **1993**, *26*, 2612.
- (13) Sakaguchi, M.; Shimada, S.; Hori, Y.; Suzuki, A.; Kawaizumi, F.; Sakai, M.; Bandow, S. *Macromolecules* **1995**, *28*, 8450.
- (14) Shimada, S.; Suzuki, A.; Sakaguchi, M.; Hori, Y. *Macromolecules* **1996**, *29*, 973.
- (15) Yamamoto, K.; Shimada, S.; Tsujita, Y.; Sakaguchi, M. *Polymer* **1997**, *38*, 6327.
- (16) Sakaguchi, M.; Shimada, S.; Yamamoto, K.; Sakai, M. *Macromolecules* **1997**, *30*, 3620.
- (17) Yamamoto, K.; Shimada, S.; Sakaguchi, M.; Tsujita, Y. *Macromolecules* **1997**, *30*, 6575.
- (18) Sakaguchi, M.; Shimada, S.; Yamamoto, K.; Sakai, M. *Macromolecules* **1997**, *30*, 8521.
- (19) Sakaguchi, M.; Yamamoto, K.; Shimada, S. *Macromolecules* **1998**, *31*, 7829.
- (20) Yamamoto, K.; Suenaga, S.; Shimada, S.; Sakaguchi, M. *Polymer* **2000**, *41*, 6573.
- (21) Sakaguchi, M.; Yamamoto, K.; Miwa, Y.; Hara, S.; Sugino, Y.; Okamoto, S.; Sakai, M.; Shimada, S. *Macromolecules* **2004**, *37*, 8128.
- (22) Sakaguchi, M.; Sohma, J. *J. Appl. Polym. Sci.* **1978**, *22*, 2915.
- (23) Yamamoto, K.; Shimada, S.; Tsujita, Y.; Sakaguchi, M. *Macromolecules* **1997**, *30*, 1776.
- (24) Sakaguchi, M.; Sohma, J. *J. Polym. Sci., Polym. Phys. Ed.* **1975**, *13*, 1233.
- (25) Heinzer, J. *Mol. Phys.* **1971**, *22*, 167.
- (26) Iwasaki, M.; Sasaki, Y. *J. Polym. Sci., Part A-2* **1968**, *6*, 1968.
- (27) Kevan, L.; Schlick, S. *J. Phys. Chem.* **1986**, *90*, 1998.
- (28) Kurokawa, N.; Sakaguchi, M.; Sohma, J. *Polym. J.* **1978**, *10*, 93.
- (29) Sakaguchi, M.; Kashiwabara, H. *J. Polym. Sci., Polym. Lett. Ed.* **1980**, *18*, 563.
- (30) Sakaguchi, M.; Yamamoto, K.; Shimada, S.; Sakai, M. *J. Polym. Sci., Part B: Polym. Phys.* **1998**, *36*, 2095.
- (31) Yamamoto, K.; Shimada, S.; Sakaguchi, M. *Polym. J.* **1997**, *29*, 370.
- (32) *CRC Handbook of Chemistry and Physics*, 76th ed.; Lide, D. R., Ed.; CRC Press: Boca Raton, FL, 1995–1996; pp 9–31.
- (33) Yoon, D. Y.; Sundararajan, P. R.; Flory, P. J. *Macromolecules* **1975**, *8*, 776.
- (34) *CRC Handbook of Chemistry and Physics*, 76th ed.; Lide, D. R., Ed.; CRC Press: Boca Raton, FL, 1995–1996; pp 13–7.
- (35) Tanaka, K.; Hashimoto, K.; Kajiyama, T.; Takahara, A. *Langmuir* **2003**, *19*, 6573.
- (36) Kajiyama, T.; Tanaka, K.; Takahara, A. *J. Polym. Sci., Part A: Polym. Chem.* **2004**, *42*, 639.
- (37) Abe, A.; Jernigan, R. L.; Flory, P. J. *J. Am. Chem. Soc.* **1966**, *88*, 631.
- (38) Bullock, A. T.; Cameron, G. G.; Smith, P. M. *J. Phys. Chem.* **1973**, *77*, 1635.
- (39) Pilar, J.; Labsky, J.; Marek, A.; Budil, D. E.; Earle, K. A.; Freed, J. H. *Macromolecules* **2000**, *33*, 4438.
- (40) Waldow, D. A.; Ediger, M. D.; Yamaguchi, Y.; Matsushita, Y.; Noda, I. *Macromolecules* **1991**, *24*, 3147.

MA062472P